Catalytic hydrotreatment of pyrolysis liquids and fractions

Yin, Wang

Chapter 3

Mo Promoted Ni Based Catalysts for the Catalytic Hydrotreatment of Pyrolysis Liquids

To be submitted to a thematic issue of ***Biomass Conversion and Biorefinery*** as an invited paper

Abstract

Catalytic hydrotreatment is a promising technology to convert pyrolysis liquids into intermediates with improved properties. Here, we report a catalyst screening study on the catalytic hydrotreatment of pyrolysis liquids using bi- and tri-metallic nickel based catalysts in a batch autoclave (initial 140 bar H_2 and 350 ^{0}C; each experiment for 4 h). The catalysts are characterized by an high nickel metal loading (41 to 57 wt.%), promoted by Cu, Pd, Mo and/or combination thereof, in a SiO_2, SiO_2-ZrO_2, or SiO_2-Al_2O_3 matrix. The hydrotreatment results are compared with a benchmark Ru/C catalyst. The results revealed that the monometallic Ni catalyst is less active and that particularly the use of Mo as the promoter is favored when considering activity and product properties. It yields a product oil with the highest H/C molar ratio and the lowest coking tendency. A drawback is the relatively high methane yield, which is close to that of Ru/C. ^{1}H, ^{13}C-NMR, HSQC and GC × GC of the product oils reveal that representative component classes of the sugar fraction of pyrolysis liquids like carbonyl compounds (aldehydes and ketones, and carbohydrates) are converted. The pyrolytic lignin fraction is less reactive, though some degree of hydrocracking is observed.

Keywords: pyrolysis liquids, nickel based catalysts, batch autoclave, hydrogenation

1. Introduction

Lignocellulosic biomass is the only sustainable resource containing carbon that can be transformed into an alternative for fossil derived crude oil and derivatives [1]. Biomass, however, has a lower energy density compared to fossil derived liquid products and, besides, scattered while collection is costly. More complicating, lignocellulosic biomass also shows considerable differences in structure and composition. It is thus imperative to develop efficient liquefaction methods to increase the energy density and as such to decrease the costs of transportation [2].

Fast pyrolysis is a technology to convert solid biomass to mainly liquid products. In the process hot vapors are generated that are quickly quenched into a liquid product. The condensable liquids are up to 70 wt% based on dry biomass feed, and are referred to as pyrolysis liquids (PLs) , bio-oils, pyrolysis oils or bio-crudes [3]. PLs contain a high amount of oxygenated components, e.g. water, acids, alcohols, aldehydes, ketones, sugar monomers and oligomers, lignin monomers and oligomers [3, 4]. The presence of acids is an issue as it leads to corrosion of for instance pipes, valves and critical parts in diesel engines (e.g. injectors) [5]. More importantly, and partially due to the high oxygen content, the thermal stability of the pyrolysis liquids is limited. Reactive oxygenated compounds, e.g. aldehydes, ketones and sugars, are the main cause of the observed increase in viscosity during storage [6, 7], due to polymerisation reactions, which take place even at low temperatures [2]. These carbonyl-containing components are also expected to lead to char formation upon processing of PLs. [7]. As such, there is an incentive to upgrade PLs and particularly to reduce acidity, and to increase the storage stability to broaden the application range. Examples of such upgrading processes are catalytic hydrotreatment [8-10], high pressure thermal treatment (HPTT) [11] and zeolite cracking [12].

During the catalytic hydrotreatment, the PLs are subjected to elevated temperatures under relatively a high pressure of H_2 in the presence of a suitable catalyst [10, 13-15]. The process severity (temperature, pressure) is of importance to steer product properties (oxygen content, water content, thermal stability). Three types of hydrogenation catalysts have been reported for the catalytic hydrotreatment of PLs. Conventional hydrodesulfurization catalysts, e.g. sulfided NiMo and CoMo on γ-Al_2O_3, have been tested extensively but, while full deoxygenation is possible [16], these catalysts appear rather unstable in time. Recently, noble metal catalysts, including Ru, Pd, Pt, Rh, on various supports (Al_2O_3, TiO_2, active carbon, ZrO_2, *etc.*) [15, 17] have

been introduced that may be less pronounced to deactivation. Ru/C was found to be superior compared to the classical hydrotreating catalysts with respect to oil yield (up to 60 wt.%) and deoxygenation level (up to 90 wt.%) [15]. Ru/C was used in extensive studies and it was shown that an initial low temperature stage (< 200°C) is advantageous to reduce char formation and to avoid rapid blockage of the reactor. Based on these findings, a reaction network was proposed [2], including hydrogenation, hydrocracking/hydrodeoxygenation and repolymerization reactions. It was shown that particularly in the initial low temperature stage of the reaction, reactive aldehydes and ketones (including carbohydrates) are converted to alcohols. A competing reaction is the thermal repolymerisation of such molecules to oligomers and finally to char. As such, it is of prime importance to identify catalysts that are particularly active in this initial stage of the reaction.

To reduce catalysts cost, there is also a clear incentive to use non-noble metal based catalyst formulations. Examples are non-sulfided Co-Mo-B and Ni-Mo-B catalysts and transition metal (Ni, Fe, Mo, Co, W) phosphides supported on silica, which have been tested for pyrolysis liquid model compounds. Hydrodeoxygenation of phenol and cyclopentanone using such catalysts yielded up to 93 % of fully deoxygenated products [18-21]. The rate of hydrodeoxygenation of guaiacol was shown to follow the order: Ni_2P > Co_2P > Fe_2P, WP, MoP [22]. The positive effect of B and P additives on catalyst activity was observed in both cases, but again, catalysts deactivate due to the loss of active components during the reaction.

Recently, we reported the use of bimetallic Ni-Cu catalysts supported on δ-Al_2O_3, CeO_2-ZrO_2, ZrO_2, SiO_2, TiO_2, rice husk carbon and sibunit for the catalytic hydrotreatment of PLs [23]. Though product oils with improved properties were obtained, char was still formed, indicating that the hydrogenation rate at low temperatures is not sufficient. Subsequently, a bimetallic Ni-Cu catalyst [24] was tested in a packed bed set-up for the catalytic hydrotreatment of pyrolysis liquids. The catalyst was characterized by a high nickel loading (57.9 wt%, 7.0 wt.% of Cu and 35.1 wt.% of SiO_2). The catalyst showed good activity at low temperature compared to the benchmark Ru/C as well as the supported NiCu catalysts with a lower Ni loading and polymerization was suppressed to a large extent.

In a later study, we reported the synthesis and application of Ni based catalysts promoted by Cu and Pd for the catalytic hydrotreatment of PLs at 350 °C in a batch autoclave. [25] Products with a high H/C ratio and low coking tendency were

observed. Ni based catalysts with Pd as the promoter were shown to be favored compared to Cu, but, as Pd is much more expensive than Cu, the potential of such Pd promoted catalysts is limited.

Motivated by the performance of Pd and Cu doped Ni based catalysts, we here report a catalyst screening study with Ni based catalysts promoted particularly by Mo for the catalytic hydrotreatment of PLs (350 ^{0}C, 140 bar H_2) in a batch autoclave. Both bi and tri-metallic catalyst Ni based catalysts were prepared and tested with Mo as well as Cu and Pd as promotors. In addition, performance was compared to the benchmark noble metal Ru/C catalyst. The product oils were analyzed by various techniques such as elemental analysis, GPC, TGA, ^{1}H, ^{13}C-NMR, HSQC and GC × GC analysis to determine relevant product properties as well as to gain insights in the molecular transformations occurring during the catalytic hydrotreatment process.

2. Experimental section

2.1 Materials

The pine wood derived pyrolysis liquid feed was supplied by the Biomass Technology Group (BTG, Enschede, the Netherlands). Relevant properties of the PL were determined and the results are given in Table 1.

Table 1 Relevant properties of the PL used in this study

Property	Pyrolysis liquid (PL)
Water content (wt%)	22.5
Elemental composition on dry basis (wt%)	
C	64.0
H	6.8
O (by difference)	29.2
N	<0.01
H/C, molar, dry	1.28
O/C, molar, dry	0.34

Hydrogen, nitrogen and helium were obtained from Linde and were all of analytical grade (> 99.99%). A reference gas containing H_2, CH_4, ethylene, ethane, propylene, propane, CO and CO_2 with known composition for gas phase calibration was purchased from Westfalen AG, Münster, Germany. Ru/C (5 wt% metal loading) was purchased from KaiDa Technology Limited, UK. Tetrahydrofuran (THF, anhydrous), di-*n*-butyl ether (DBE, anhydrous, 99.3%), Dimethyl sulfoxide-d6 (99.6 atom % D), chloroform-d_1 (99.96 atom % D), $CaCl_2$ (anhydrous, ≥ 93.0%) were purchased from Sigma-Aldrich and used without further purification, levoglucosan was supplied from Carbosynth, UK and used as received.

2.2 Catalyst synthesis and composition

The catalysts were prepared using a sol-gel methodology according to a procedure given by Bykova *et al.* [26-29] The amounts of active metals, supports and activation parameters are summarized in Table 2. The catalysts were crushed and sieved, and the fraction between 25 and 75 μm was used for the hydrotreatment reactions.

Table 2 Summary of the properties of catalysts used in this study[a]

Code	Metal Loading, wt%				Support, wt%			Reduction temperature, °C/time, h
	Ni	Cu	Mo	Pd	SiO_2	Al_2O_3	ZrO_2	
Ni monometallic	49	~	~	~	16.6	~	21	350/1
Ni-Cu	46	5	~	~	25	~	10.7	350/1
Ni-Pd	57	~	~	0.7	26	~	~	350/1
Ni-Pd-Cu	54	8.2	~	0.7	21	~	~	350/1
Ni-Mo-Cu	38	3.8	5.9	~	10.8	24	~	400/1
Ni-Mo	41	~	7.4	~	13.3	24	~	400/1

[a] Oxidized form

2.3 Experimental procedures

2.3.1 Catalytic hydrotreatment of pyrolysis liquids in a batch autoclave

Catalysts screening experiments were performed in a 100 ml Parr autoclave equipped with an overhead stirrer. Prior to the experiment, the reactor was charged with 1.25 g of catalyst (5 wt% with respect to pyrolysis liquids feed). Subsequently, the reactor was pressurized with 100 bar of N_2 to check for leakage. The catalyst was then pre-reduced using 20-30 bar H_2 at a temperature of 350 °C (400 °C for Ni-Mo/SiO_2-Al_2O_3, Ni-Cu-Mo-P/SiO_2-Al_2O_3) for 1 h. Subsequently, the reactor was cooled to room

temperature and 25.0 g of the PL was injected to the reactor from a feed vessel using pressurized nitrogen gas. Then the reactor was flushed 3 times with 10 bar of hydrogen to remove air, and was subsequently pressurized to 140 bar at room temperature. Finally, the reactor was heated to 350 ^{o}C with a heating rate of around 10 ^{o}C/min at a stirring speed of 1400 rpm. The reaction was allowed to proceed at 350 ^{o}C for 4 h. Then, the reactor was cooled to ambient temperature and the pressure in the reactor was recorded for mass balance calculations, the reactor was vented and the gas phase was collected in a 3 L gas bag. The reactor content (liquids and spent catalyst) were collected and transferred to a centrifuge tube and weighed. The liquid phases (water and product oil) were separated by centrifugation (4500 rpm, 30 min) and both phases were collected and weighted. The reactor was thoroughly rinsed with acetone. The acetone phase was evaporated in air, and the resulting product was weighted and added to the organic phase and used as input for the mass balance calculations. The remaining solid residue combined with the solid residue in the centrifuge tube was filtered over a paper filter, washed with acetone and dried at 100 ^{o}C till constant weight. The amount of char is defined as the amount of solid residue minus the original catalyst intake. The amount of gas phase after reaction was determined by the pressure difference in the reactor before and after reaction at room temperature using the ideal gas law, assuming that the volume of the gas hold-up in the reactor before and after reaction was constant. A detailed procedure is given in previous studies [17, 30].

2.3.2 Product analysis

GC-TCD. The composition of the gas phase after reaction was determined by GC-TCD. A Hewlett Packard 5890 Series II GC equipped with a CP Poraplot Q Al_2O_3/Na_2SO_4 column (50 m × 0.5 mm, film thickness 10 μm) and a CP-molsieve (5Å) column (25 m × 0.53 mm, film thickness 50 μm) was used. The injector temperature was set at 150 ^{o}C, the detector temperature at 90 ^{o}C. The oven temperature was kept at 40 ^{o}C for 2 min, then heated up to 90 ^{o}C at 20 ^{o}C/min and kept at this temperature for 2 min. Helium was used as the carrier gas. The columns were flushed for 30 s with (reference and sample) gas before starting the measurement. A reference gas containing H_2, CH_4, CO, CO_2, ethylene, ethane, propylene and propane with known composition was used for peak identification and quantification.

Elemental Analysis. The elemental compositions of the PL feed and product oils

were analyzed by elemental analysis using an EuroVector EA3400 Series CHNS-O with acetanilide as the reference. The oxygen content was determined by difference. All analyses were carried out at least in duplicate and the average value is reported.

Water Content. The water content of the PL feed and product oils were determined using a Karl-Fischer (Metrohm 702 SM Titrino) titration. About 0.01 g of sample was introduced to an isolated glass chamber containing Hydranal solvent (Riedel de Haen) by a 1 ml syringe. The titration was carried out using Hydranal titrant 5 (Riedel de Haen). Milli-Q water was used for calibration. All analyses were carried out at least in duplicate and the average value is reported.

Gel Permeation Chromatography (GPC). GPC analyses of the PL feed and product oils were performed using an Agilent HPLC 1100 system equipped with a refractive index detector. Three columns (mixed type E, length 300 mm, i.d. 7.5 mm) in series of were used. Polystyrene was used as a calibration standard. 0.05 g of the organic phase was dissolved in 5 ml of THF (10 mg/ml) together with 2 drops of toluene (flow marker) and filtered (pore size 0.2 μm) before injection.

Thermogravimetric Analysis (TGA). TGA data of the PL feed and product oils were obtained using a TGA 7 from Perkin-Elmer. The samples were heated in a nitrogen atmosphere with a heating rate 10 ^{o}C/min between 20-900 ^{o}C.

Gas Chromatography/Mass Spectrometry (GC-MS). GC-MS analyses of the liquid products were performed on a Hewlett-Packard 5890 gas chromatograph equipped with a quadrupole Hewlett-Packard 6890 MSD selective detector and a 30 m × 0.25 mm, i.d. and 0.25 μm film sol-gel capillary column. The injector temperature was set at 250 ^{o}C. The oven temperature was kept at 40 ^{o}C for 5 min, then increased to 250 ^{o}C at a rate of 3 ^{o}C/min, and then held at 250 ^{o}C for 10 min. Di-*n*-butyl ether was used as an internal standard for quantification of relevant components in the PLs and products.

Two-Dimensional Gas Chromatography (GC × GC). GC × GC-FID analysis was performed on product oils and the PL feed with a trace GC × GC from Interscience equipped with a cryogenic trap system and two columns: a 30 m × 0.25 mm i.d. and a 0.25 μm film of the RTX-1701 capillary column connected by using a meltfit to a 120 cm × 0.15 mm i.d. and a 0.15 μm film Rxi-5Sil MS column. An FID detector was used. A dual jet modulator was applied using carbon dioxide to trap the samples. Helium was used as the carrier gas (continuous flow 0.6 ml min^{-1}). The injector temperature and FID temperature were set at 250 °C. The oven temperature

was maintained at 40 °C for 5 minutes then heated up to 250 °C at a rate of 3 °C min^{-1}. The pressure was set at 70 kPa at 40 °C. The modulation time was 6 s. For GC × GC-FID and GC-MS-FID analyses, the samples were diluted with tetrahydrofuran (THF) and 500 ppm di-n-butyl ether (DBE) was added as an internal standard. Detailed procedures regarding calibration and quantification are described in previous studies [31-33].

^{1}H-, ^{13}C-NMR. For ^{1}H-NMR, around 10 mg of the PL feed or the product oils was dissolved in 1.0 g of $CDCl_3$. The sample was dried by passing it over a short column containing $CaCl_2$. For ^{13}C-NMR, 0.5 g of sample was dissolved in 0.5 g of DMSO-d_6. The NMR spectra were recorded on a Varian AS400 spectrometer.

Heteronuclear Single Quantum Coherence (HSQC) NMR. NMR spectra were acquired at 25 °C using an Agilent 400 MHz spectrometer. Approximately 0.5 g of sample was dissolved in 0.5 g of DMSO-d_6. ^{1}H–^{13}C HSQC spectra were acquired using a standard pulse sequence with a spectral width of 160 ppm, 16 scans and 256 increments in the F1 dimension. The data were processed using the MestReNova software.

2.4 Definitions

The hydrogen consumption during reaction was calculated according to a method reported in previous studies from our group and quantified using Eq. (1) [17, 30]. The hydrogen consumption corrected for methane formation was calculated using Eq. (2). Here it is assumed that all the bound hydrogen in methane is derived from the hydrogen feed.

$$H_2\ consumption = \frac{(n_{H_2,\,initial} - n_{H_2,\,final})}{m_{PL,\,initial}} \cdot 22.4 \qquad (1)$$

$$H_2\ consumption\ corrected\ \ for\ methane = H_2\ consumption - (2 \cdot n_{methane} \cdot 22.4) \qquad (2)$$

where the $H_2\ consumption$ is the hydrogen uptake (in NL per kg feed), $n_{H_2,\,initial}$ is the initial amount of hydrogen (in moles) in the reactor, $n_{H_2,\,final}$ is the amount of hydrogen (in moles) in the reactor after the reaction, R is the gas constant, $m_{PL,\,initial}$ is the mass of the pyrolytic liquid fed to the reactor. $n_{methane}$ is the amount of methane

formed (in moles) in the reactor, 22.4 is standard volume of 1 mole of an ideal gas at standard temperature and pressure.

3. Results and discussions

3.1 Product distribution

Catalytic hydrotreatment reactions were performed over six Ni based catalysts, either Ni as such (monometallic) or promoted by Cu, Pd and Mo (bi-metallic) and combinations thereof. Detailed catalyst compositions are given in Table 2. The catalysts were pre-reduced before reactions. For comparison, experiments were carried out with Ru/C, a benchmark noble metal catalyst. Reactions were performed in a batch set-up at standard conditions (350 ^{o}C, 4 h, 140 bar H_2 at the start of the reaction).

The hydrotreatment procedure always resulted in the formation of two separate liquid phases, an aqueous and an organic product phase. For Ru/C, Ni-Mo-Cu and Ni-Mo, the product phase has a density lower than water, while for the other catalysts the product appeared as the bottom phase. The oxygen content in the product oils for the Ni based catalysts are in a narrow range and between 13 to 15 wt%. As such, full hydrodeoxygenation at the conditions applied in this study is not taking place, in line with earlier studies using Ni based catalysts. [25, 34] For Ru/C, the oxygen content is the lowest, below 10 wt%. For all product phases, the water content is below 5 wt%, with only minor deviations between the catalysts (Table 3).

The amounts of gaseous, organic, aqueous, and solid phases are shown in Table 3. Mass balance closures are > 92% for all catalysts. The amounts of organic phases were between 41.5 and 53.1 wt% on feed, whereas the amounts of the aqueous phases were between 35.1 and 42.9 wt% on feed. Solids formation appears very low for all catalysts, and is generally below 0.7 wt%. These values are lower than reported in our previous studies on the catalytic hydrotreament of PLs using Ni based catalysts (1.2-2.4 wt%) [25, 34] at 350 ^{o}C. These differences may be related to the slightly different experimental procedures used in both studies as well as differences in the properties on the PL feeds used (e.g. water content, coking tendency).

Table 3 Overview of catalytic hydrotreatment experiments using Ni-based catalysts

Catalysts	Ru/C	Ni monometallic	Ni-Cu	Ni-Pd	Ni-Pd-Cu	Ni-Mo-Cu	Ni-Mo
Organic Phase (wt% on PL intake)	41.5	52.7	49.5	52.5	53.1	43.2	42.4
Aqueous Phase (wt% on PL intake)	42.9	37.8	38.8	36.0	35.1	40.2	41.5
Solids (wt% on PL intake)	0.1	0.7	0.3	0.1	-	-	0.1
Gas phase (wt% on PL intake)	9.4	5.8	6.7	5.9	5.9	9.8	8.3
Carbon dioxide (mol%)	14.2	8.1	9.0	8.0	7.8	15.6	15.3
Ethane (mol%)	2.5	0.6	1.2	0.7	0.7	4.5	5.4
Propane (mol%)	1.5	0.4	0.8	0.5	0.5	3.0	3.1
Hydrogen (mol%)	54.3	86.9	68.0	84.0	84.8	49.5	56.2
Methane (mol%)	27.5	3.4	20.7	5.5	4.3	27.0	20.0
Carbon monoxide (mol%)	0.0	0.7	0.0	1.3	1.8	0.4	0.0
Mass Balance closure (%)	93.9	97.1	95.2	94.4	94.2	93.2	92.4
Hydrogen uptake, Nl/kg PL	299	200	276	219	216	317	312
Hydrogen uptake corrected for CH_4, Nl/kg PL	211	187	212	198	201	230	259
Water content of organic phase, wt%	4.4	5.2	4.6	4.7	5.6	2.9	2.9
Elemental composition of organic phase (dry)							
C	81.43	75.86	76.01	75.15	75.81	77.15	77.21
H	9.53	9.08	9.16	9.28	9.27	9.48	9.55
O	9.04	15.06	14.83	15.57	14.92	13.37	13.23
Ccarbon balance closure, %	89.4	98.8	95.5	98.2	99.4	90.7	88.0
Carbon in gas phase, %	10.2	3.7	6.7	4.2	4.2	11.1	9.1
Carbon in aqueous phase, %	4.7	7.5	6.0	7.1	7.4	4.9	5.3
Carbon in oil phase, %	74.5	87.6	82.8	86.9	87.8	74.7	73.5

The gas phase still contained up to 50 mol% of hydrogen, suggesting that the reactions were not carried out under hydrogen starvation conditions. The main gas products are CO_2 and small alkanes (particularly CH_4 and some C_2-C_3 hydrocarbons). CO_2 is known to be formed by amongst others, the decarboxylation of the organic acids in the PL feed, and particularly from formic acid [9]. CH_4 is either from gas phase reactions like the methanation of CO_2 and CO [35] or from liquid phase reactions, for instance by aqueous phase reforming of organics [36] and demethoxylation of the lignin fractions in the PL feed [25]. Methanation by gas phase reactions is an undesired reaction as it reduces the carbon efficiency of the process and leads to higher consumption levels of (expensive) hydrogen.

Methane formation appears a strong function of the catalyst composition. For the monometallic Ni and the Pd promoted catalysts (Ni-Pd and Ni-Pd-Cu), the amount of methane in the gas phase is below 5 mol%. For the Cu and Mo promoted catalysts significantly more methane is present (up to 27 mol% in the gas), close to the Ru/C (27.5 mol%) catalyst, which is a known methanation catalyst [24]. Earlier studies on Ni-Cu catalyst with a high Ni loading (57.9 wt%) with SiO_2 as the matrix gave by lower rate of methanation (0.2 mol/kg $_{PL}$) compared to the catalyst used here (2.3 mol /kg $_{PL}$). The main difference in catalyst composition is the inorganic matrix, viz. SiO_2 versus a SiO_2-ZrO_2 matrix here. ZrO_2 is known to promote the demethoxylation of the guaiacol and syringol units in the lignin fractions to form CH_4 [25] and this could explain the differences in methanation rates between both catalysts.

The carbon balances for the various catalysts are given in Table 3 and Figure 1. For this purpose, the elemental composition of the gas and both liquid phases were determined. Carbon balance closures are between 88 and 99%, the lower values for some of the experiments are caused by inaccuracies in weight determination of the organic phase. This is particularly cumbersome in the case a top oil is produced.

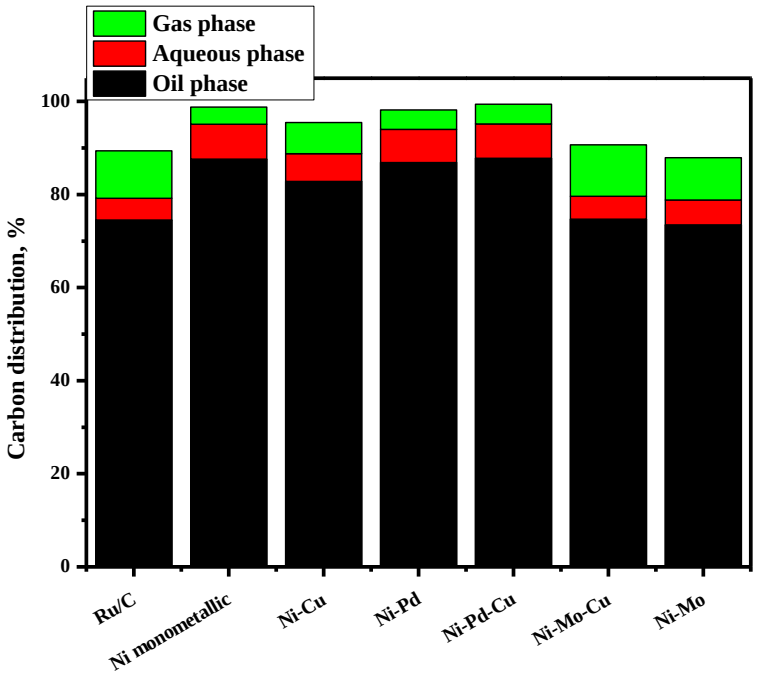

Figure 1 Organic carbon distribution for the catalytic hydrotreatment of PLs using Ni based catalysts and Ru/C at 350 ^{o}C for 4 h

Most of the carbon is retained in the organic product phase (> 75%), with the highest values for Ni-Pd (> 87%). The value for the monometallic Ni catalyst is also in the same range, however, the product properties are not as good as for the Pd promoted catalysts (*vide infra*). The organic carbon recovery in the oil phase using the Mo promoted catalysts (see Ni-Mo and Ni-Mo-Cu) are around 75 %, similar to benchmark Ru/C catalyst. Carbon loss due to the accumulation of organics in the water phase is below 7.5 wt%.

3.2 Activity of the catalysts

The experimentally determined hydrogen consumption is a good measure for catalytic activity. [17, 30] However, in the case of extensive methane formation, the activity for liquid phase reactions (hydrogenation, hydrodeoxygenation and hydrocracking) is overestimated when using this procedure. As such, the hydrogen consumption was corrected for methanation reactions (see experimental section for calculation details) and the results are given in Figure 2.

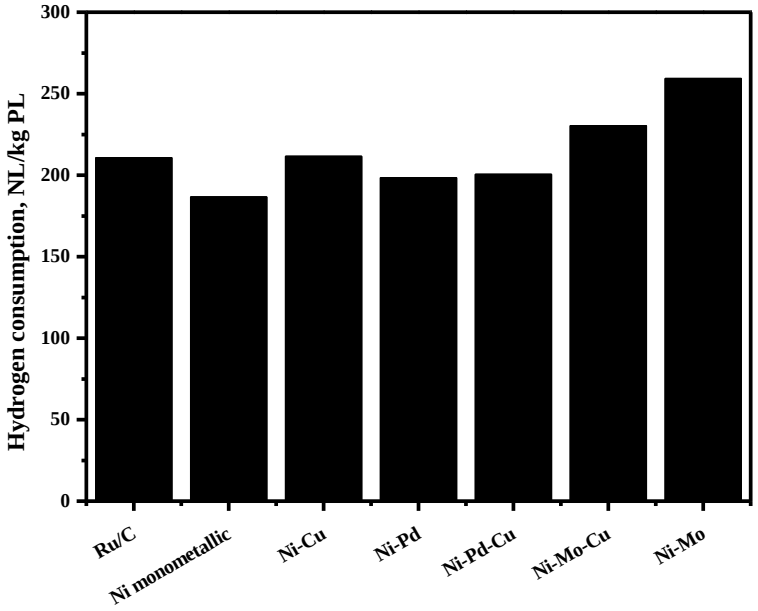

Figure 2 Hydrogen consumption (corrected for methane formation) for the Ni based catalysts and Ru/C

The Mo promoted Ni catalysts show the highest hydrogen consumption (about 260 Nl/kg PL feed), whereas the monometallic Ni catalysts is the least active (187 Nl/kg PL feed). Thus, Mo addition has a clear positive effect on the activity of the catalysts. The addition of Cu to Ni based catalysts increases the hydrogen consumption, which is consistent with our previous studies, e.g. hydrogenation of sugar rich fractions of pyrolysis liquids at 180 ^{o}C [37] and whole pyrolysis liquids at 350 ^{o}C [25]. Pd addition also has a positive effect on the catalysts activity, resulting in higher hydrogen consumptions compared to monometallic Ni catalyst.

3.3 Composition of the organic phase

A van Krevelen plot with the elemental composition of the PL feed and the product oils obtained with all catalysts is shown in Figure 3. The H/C molar ratio of the PL feed is around 1.27, the value for the product oils using Ni based catalysts are all higher and in the range of 1.44 to 1.49. The O/C ratio of the product oils is considerably lower (0.10-0.15) than for the PL feed (0.35), though essentially similar for all Ni based catalysts.

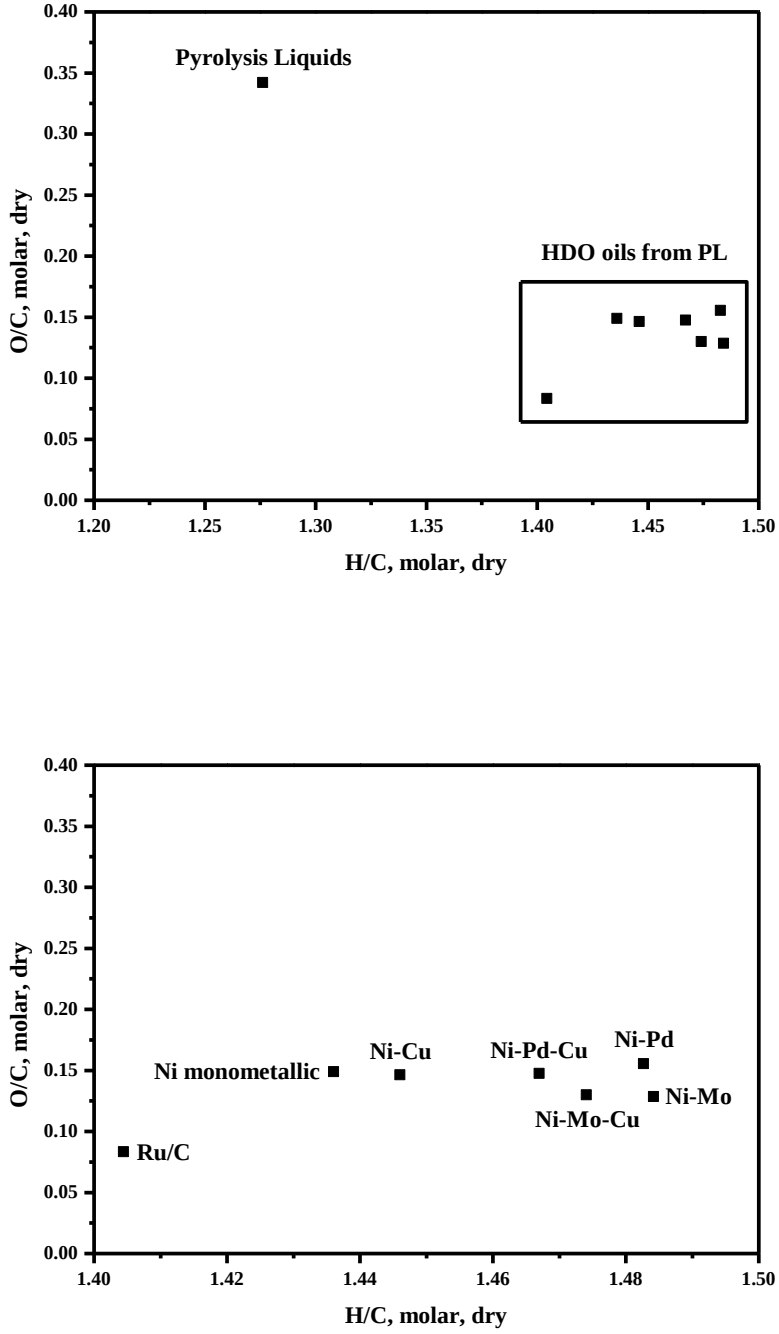

Figure 3 van Krevelen plot for the PL feed and products oils after a catalytic hydrotreatment reaction using the Ni based catalysts and Ru/C (350 ^{o}C, 4 h)

Interestingly, a higher H/C ratio is observed for all oils produced over Ni based catalysts compared to the benchmark Ru/C catalyst. Higher H/C ratios are indicative for a product with improved product properties such as a higher thermal stability (lower coke formation upon heating). As such, the product oils using the Ni based

catalysts are expected to be preferred compared to those obtained with Ru/C. On a molecular level, it implies that the Ni catalysts are more active hydrogenation catalysts, particularly in the early stage of the reaction than Ru/C.

The H/C ratio for the Ni based catalysts shows some variations (Figure 3). The monometallic Ni catalyst yielded a product oil with the lowest H/C ratio among all the Ni based catalysts. Cu addition to the Ni based catalysts led to a higher H/C ratio, which is in good agreement with our previous studies on the catalytic hydrotreatment of PLs [25] and sugar fractions thereof [37] using Ni-Cu based catalysts. Pd addition leads to higher H/C ratio in the product oils (see Ni-Pd and Ni-Pd-Cu), likely because Pd is a good hydrogenation catalyst [38].

The molecular weight distributions of the PL feed and the product oils were analyzed by GPC and the results are shown in Figure 4. The crude pyrolysis liquid shows a rather sharp peak at a molecular weight around 200 g/mol, which can be attributed (and confirmed by spiking) to levoglucosan (LG). The LG peak is considerably lower in the product oils, indicating that LG is converted during the catalytic hydrotreatment. [25, 34] For the product oils, the higher molecular weight tail is significantly reduced to lower values, which indicates that thermal polymerisation in the initial stage of the reaction is limited, while hydrocracking at elevated temperatures leads to a reduction of the molecular weight. The molecular tail is shifted to lower molecular weights in particular when using the Mo promoted Ni based catalysts (Ni-Mo, Ni-Mo-Cu), see Figure 4 for details. Overall, the molecular weight of the products is much lower than for the original PL feed and this implies that hydrocracking also occurs to a significant extent.

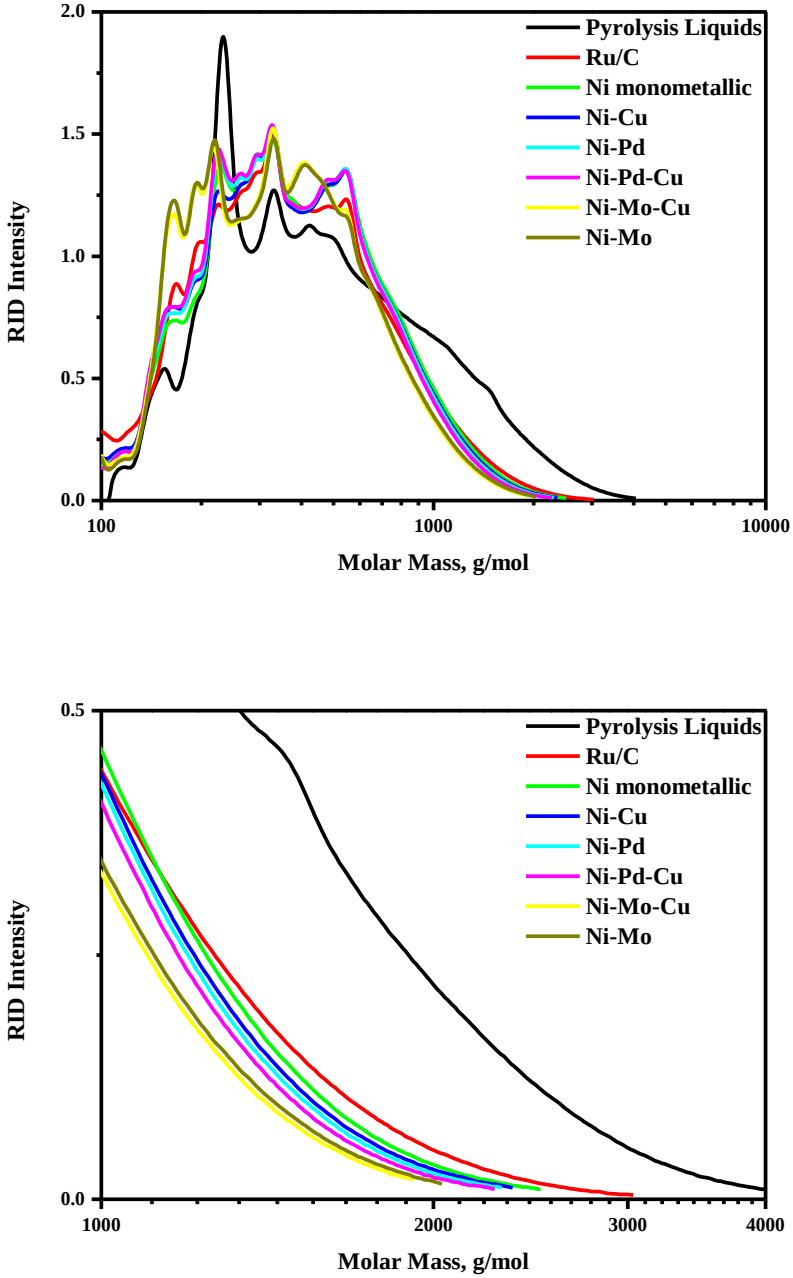

Figure 4 Molecular distribution of the PL feed and product oils over nickel based catalysts and Ru/C by GPC

Charring tendency is known to be another parameter that can be used to qualify product oils from pyrolysis processes. [25, 39] To determine the quality in terms of charring tendency, thermographimetric analysis (TGA) has shown to be a very suitable method. Specifically the residue (TG residue) after heating the sample in an

inert atmosphere till 900 oC [40] is a valuable measure as it actually resembles the MCRT value conventionally used for crude oil feeds [41].

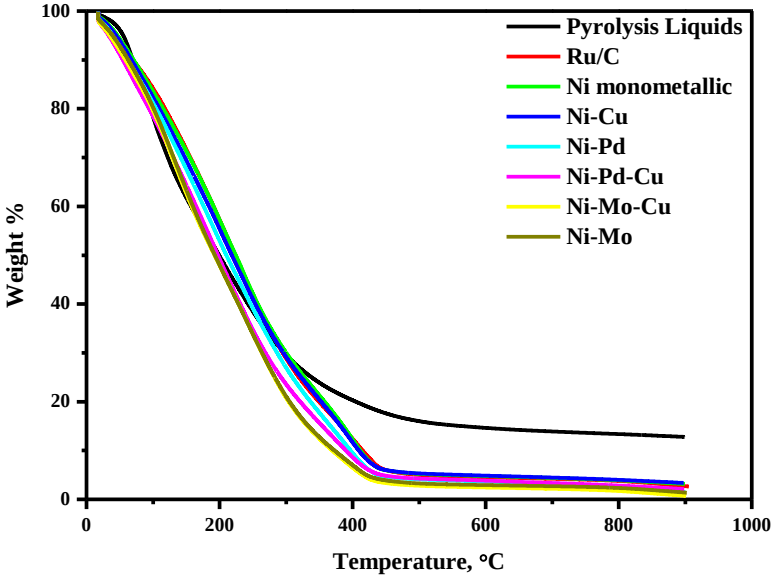

Figure 5 TGA data for the PL feed and product oils

For the PL feed, the TG residue is about 13 wt%, while it is considerably reduced below 3.5 wt%) for the product oils as shown in Figure 5 and Table 4. As such, the catalytic hydrotreatment has led to a considerable improvement in the thermal stability of the oils.

Table 4 TG residue of PL feed and product oils using the Ni based catalysts and Ru/C

Catalysts	TG residue, wt%[a]
PL feed	12.8
Ru/C	2.6
Ni monometallic	3.2
Ni-Cu	3.4
Ni-Pd	1.5
Ni-Pd-Cu	2.1
Ni-Mo-Cu	0.7
Ni-Mo	1.4

[a] Defined as the residual weight after heating the sample to 900°C in an inert atmosphere

The Mo promoted catalysts (Ni-Mo and Ni-Mo-Cu) gave the product oils with lowest TG residue (0.7-1.4 wt%), whereas the value was highest with the monometallic Ni and Ni-Cu catalysts (> 3 wt%). Thus, to obtain product oils with low TG residues, Mo promoted Ni catalysts are preferred and show better performance than the Cu and Pd promoted catalysts.

3.4 Molecular transformations

To investigate the reactions occurring during the catalytic hydrotreatment process, a typical product oil when using the Ni-Mo catalyst and the PL feed were analyzed by ^{1}H, ^{13}C-NMR, HSQC and GC × GC. The results are shown in Figures 6-8 and Table 5-6.

^{13}C-NMR spectra and the integration results for the PL feed and the product oil using the Ni-Mo catalyst are shown in Figure 6 and Table 5. Classification of the various organic groups based on NMR shifts was done using the Ingram method [42].

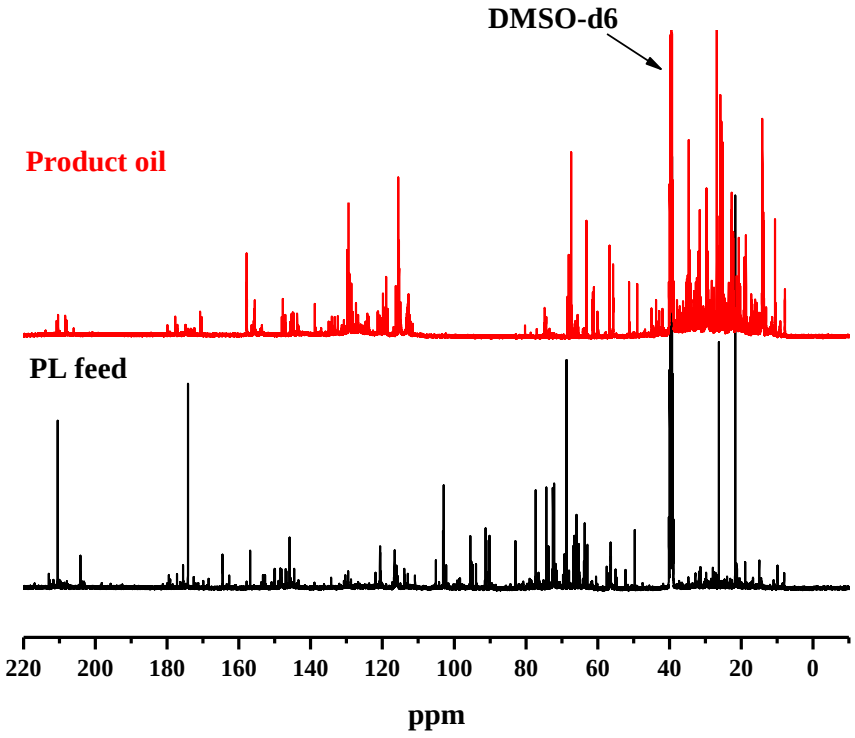

Figure 6 ^{13}C-NMR spectra of the PL feed and product oil using Ni-Mo at 350 ^{o}C for 4 h

Table 5 ^{13}C-NMR data for the PL feed and a product oil from a reaction with Ni-Mo at 350 ^{o}C for 4 h

Chemical shift region δ (ppm)	Carbon assignments	PL feed (%-C)	Product oil Ni-Mo (%-C)
215-163	Total carbonyl	6.7	1.8
215-180	Carbonyl (ketones + aldehydes)	3.8	0.5
180-163	Carbonyl (esters + carboxylic acids)	2.9	1.3
163-100	Total aromatics	15.1	7.2
163-125	General aromatics	5.6	4.2
125-112	Aromatics (guaicyl)	7.1	2.9
112-100	Aromatics (syringyl)	2.4	0.1
110-84	Carbohydrates	2.8	0.0
84-54	Methoxy/hydroxyl groups	20.1	2.0
54-1	Alkyl carbon (total)	16.8	40.1
54-36	Long/branched aliphatics	0.1	3.1
36-1	Short aliphatics	16.7	36.9

Clearly, the carbonyl compounds, especially ketones and aldehydes (δ = 163 to 215 ppm), are readily converted, while carboxylic acids/esters are still present in the product oil in considerable amounts. As such, the carboxylic acids/esters are rather inert while the aldehydes and ketones are very reactive. These results are in good agreement with our previous studies on hydrogenated oils using Ni-Cu at different temperatures [34]. The peak intensity of the resonances in the aromatic region, for a larger part arising from the aromatic units of the pyrolytic lignin fraction, decreased from 15.1 in the PL feed to 7.2% in the product oil. As such, the pyrolytic lignin fraction also shows considerable reactivity at the prevailing reaction conditions. Concomitantly, the amount of components with aliphatic carbons increases considerably, as evident from an increase in peak area in the chemical shift range between δ 1 and 54 ppm.

The resonances between δ 84 and 110 ppm arising from carbohydrates are clearly present in the PL feed. Upon the hydrotreatment, these peaks disappear, indicative for high reactivity of the carbohydrates at 350 ^{o}C.

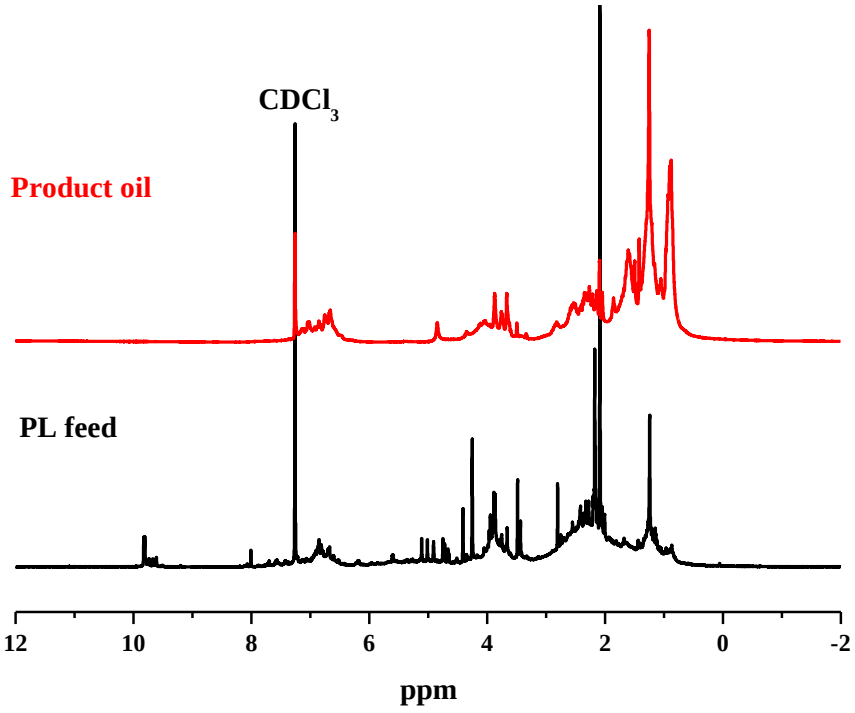

Figure 7 ^{1}H-NMR spectra of the PL feed and a product oil using Ni-Mo at 350 ^{o}C for 4 h

Table 6 ^{1}H-NMR Data for pyrolysis liquids feed and product oils using Ni-Mo at 350 ^{o}C for 4 h

Chemical shift region δ (ppm)	Proton assignments	PL feed (%-H)	Product oil Ni-Mo (%-H)
10.0-8.0	-CHO, -COOH, downfield ArH	1.7	0
8.0-6.8	ArH, HC=C (conjugated)	4.9	4.2
6.8-6.4	HC=C (nonconjugated)	2.8	3.8
6.4-4.2	$-CH_n-O-$, ArOH, HC=C (nonconjugated)	12.1	3.2
4.2-3.0	CH_3O-, $-CH_2O-$, -CHO-	17.1	9.9
3.0-2.2	$CH_3(=O)-$, CH_3-Ar, $-CH_2Ar$	22.2	13.9
2.2-1.6	$-CH_2-$, aliphatic OH	21.5	15.1
1.6-0.0	$-CH_3$, $-CH_2-$	17.6	49.9

The reactivity of the various organic component classes in the PLs was also confirmed by ^{1}H-NMR measurements. The percentages of protons of various groups in the product oils and PL feed were classified using a reported procedure by Mullen *et al.* [43] (see Figure 7 and Table 6 for details).

Aldehydes with typical resonances in the chemical shift region from δ 8.0 to 10.0 ppm are fully converted. In addition, the peak intensity of resonances arising from carbohydrates (δ 4.2-6.4 ppm) is also reduced considerably, indicative for a high reactivity of this fraction. The main products are aliphatics with resonances in the range between δ 0.0 to 1.6 ppm.

Extensively used for lignin characterization [44], we here also carried out the ^{1}H-^{13}C HSQC technique. The overlay of spectra for the crude PL feed and a typical product oil using the Ni-Mo catalyst is given in Figure 8.

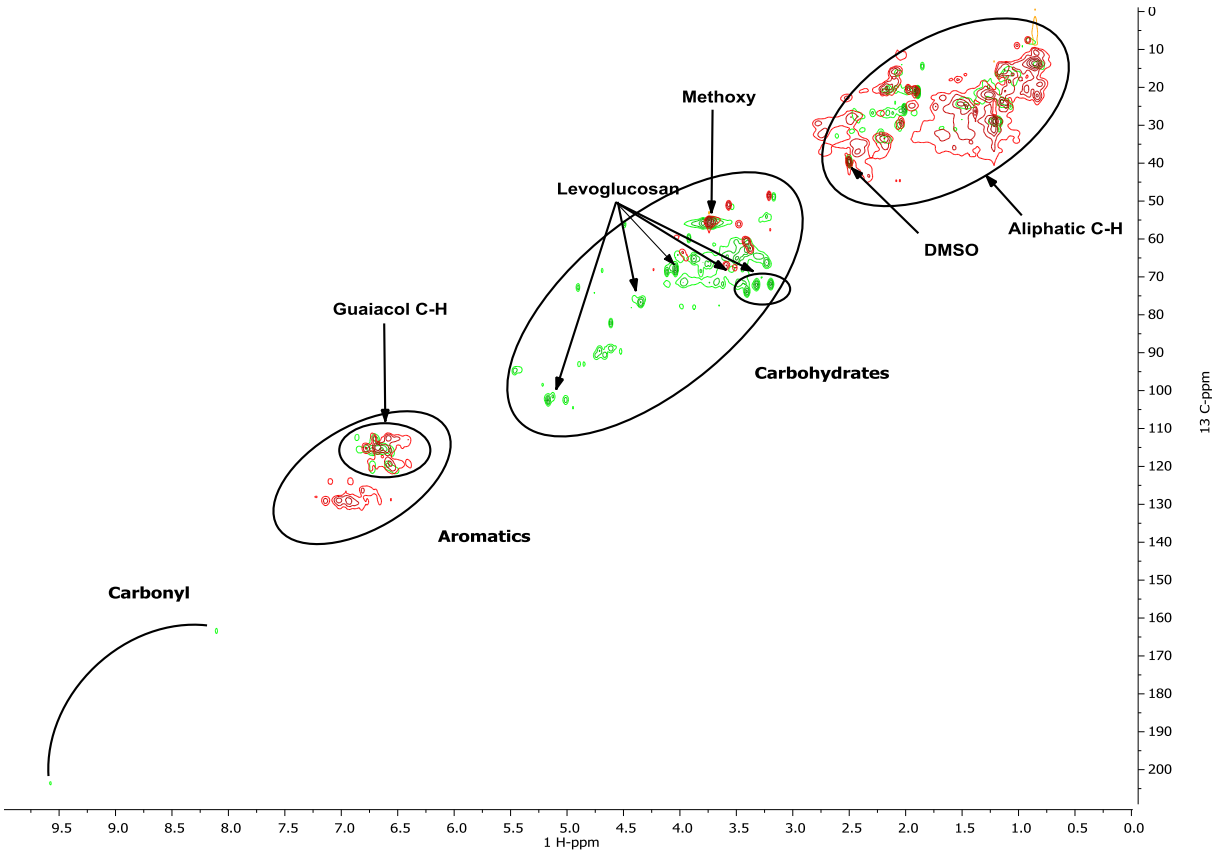

Figure 8 Heteronuclear Single Quantum Coherence (HSQC) spectra of the PL feed (green) and product oil (red) after a catalytic hydrotreatment over Ni-Mo at 350 ^{o}C for 4 h

The results supplement the separate ^{1}H and ^{13}C-NMR measurements. For instance, it shows that -OMe groups on aromatic rings arising from the lignin fraction are partly converted. In addition, major individual components can be clearly identified, the most prominent example being LG. Characteristic resonances of LG in the PL feed (Figure 8) are absent in the product oil, indicative for quantitative conversion.

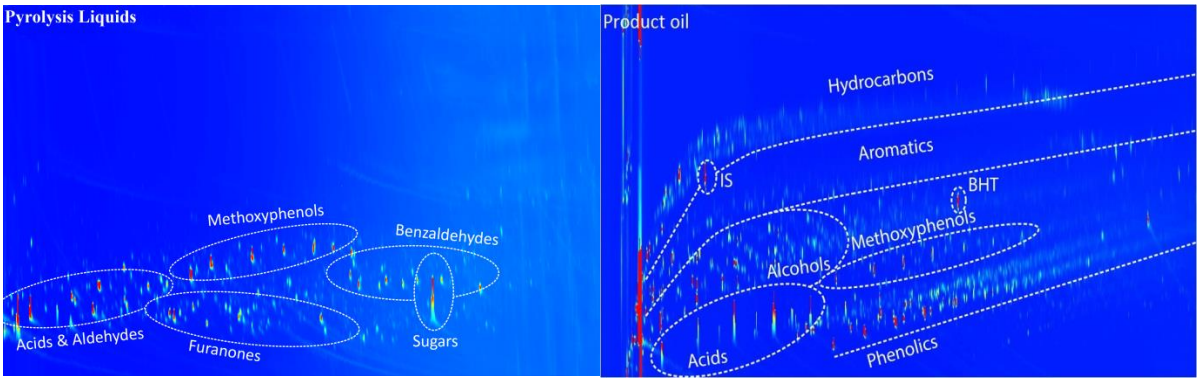

Figure 9 GC × GC spectrum of the PL feed and product oil using Ni-Mo at 350 ^{o}C for 4 h (IS is the internal standard, BHT is the stabilizer in THF).

The reactivity of aldehydes, ketones and carbohydrates as observed by NMR techniques is further confirmed by GC × GC measurements as shown in Figure 9. The amounts of phenolics, alcohols, methoxyphenolics and hydrocarbons increased to a certain extent at the expense of sugars, aldehydes and ketones. The phenolics and methoxyphenolics likely arise from the hydrocracking of the pyrolytic lignin fraction. Considerable amounts of carboxylic acids are still present in the product oil, confirming their rather inert nature. The GC × GC results are consistent with NMR results in Figure 6-8.

3.5 Catalyst selection

Suitable catalysts for the catalytic hydrotreatment lead to organic products with favorable product properties such as low charring tendency (low TG residue) and a high H/C ratio. In addition, the carbon is preferably retained quantitatively in the organic product phase. A high H/C ratio generally corresponds with a higher energy density of the product oil. Furthermore, it is known to lead to improved solubility in apolar solvents, which is advantageous when considering co-feeding of the product in FCC refinery units. A plot with the three relevant quality indicators as a function of

the catalyst composition is given in Figure 10. The preferred catalysts are in the right bottom of part the graph.

Based on this figure, the preferred catalysts regarding product properties are the Mo promoted catalysts and the Ni-Pd catalyst. When also taking into account the carbon balance, the Pd based catalysts (Ni-Pd and Ni-Pd-Cu) seem preferred (Figure 10). Considering that Pd is around 1350 times more expensive than Mo (22,000 US$/kg for Pd versus 16.3 US$/kg for Mo [45]), Mo can be considered a good promotor for these Ni based catalysts.

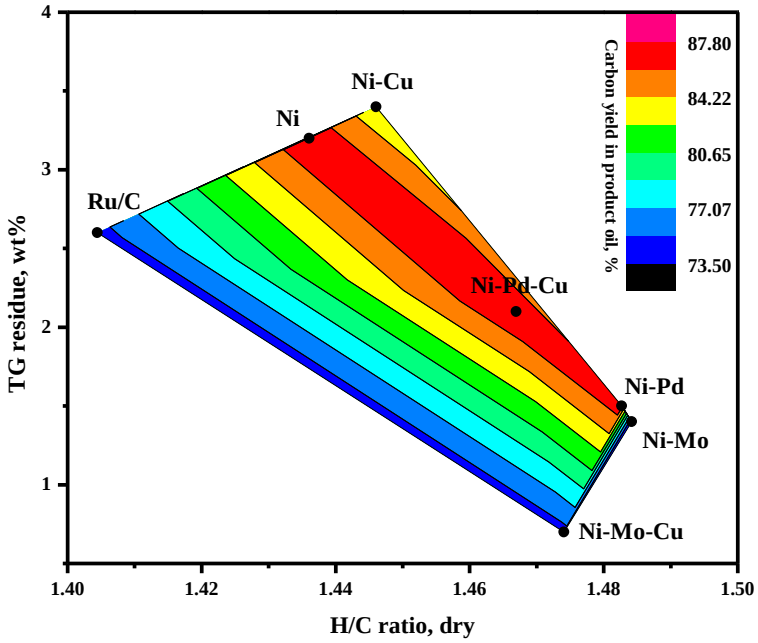

Figure 10 Quality indicators (TG residue, H/C ratio, carbon yield in product phase) for the Ni based catalysts and Ru/C

Despite these positive aspects, catalyst improvements are possible in terms of the organic carbon yields, which are lower for the Mo promoted catalysts compared to the Pd promoted ones. The main difference between Pd and Mo promoted catalysts when considering the carbon distribution over the product phases is a higher amount of methane in the gas phase for Mo. Methane is to a large extent formed by gas phase reactions of CO and CO_2. As such, modification of this catalysts to reduce the decarboxylation activity as well as the rate of subsequent gas phase reactions to methane should be a major topic for future catalyst development regarding noble metal free Ni based catalysts.

The benchmark Ru/C catalyst shows worse performance than the Ni based catalysts particularly when considering the product properties. For the monometallic Ni and bimetallic Ni-Cu catalysts the product properties are also by far worse than for Mo promoted catalysts.

Conclusions

The catalytic hydrotreatment of PLs using nickel based catalysts promoted by Cu, Pd and Mo was investigated at 350 ^{o}C. Best performance on basis of (dry product based) H/C ratio and TG residue was obtained by promotion with Mo. For these catalysts also the reaction rate, expressed as the hydrogen uptake corrected for methane formation per kg PL feed, was the highest. Carbon balance calculations show that the amount of carbon ending up in the organic product phase is actually higher for Pd (85%) than for Mo promotion (75%) due to higher methanation activity for the Mo promoted catalysts. The actual rate of methanation of the Ni-Mo catalyst is similar to the benchmark Ru/C. Further catalyst studies should be aimed to reduce methane formation. Analysis of the product oil (^{1}H, ^{13}C-NMR, HSQC and GC × GC) obtained with the Ni-Mo catalyst revealed that aldehydes, ketones and carbohydrates are readily converted, while the pyrolytic lignin fraction is more inert, though prone to hydrocracking (GPC).

Acknowledgement

Financial support from Agentschap NL (Groene aardolie via pyrolyse, GAP) is gratefully acknowledged. The authors thank Arjan Kloekhorst and Monique Bernardes Figueirêdo (Department of Chemical Engineering, University of Groningen) for NMR analysis. Hans van der Velde (Stratingh Institute for Chemistry, University of Groningen) is acknowledged for performing the elemental analyses and G. O. R. Alberda van Ekenstein (Depertment of Polymer Chemistry, Zernike Institute for Advanced Materials, University of Groningen) for TGA analysis. We also thank Leon Rohrbach, Jan Henk Marsman Erwin Wilbers, Marcel de Vries and Anne Appeldoorn for analytical and technical support.

References

[1] J.N. Chheda, G.W. Huber, J.A. Dumesic, Angewandte Chemie International Edition. 46 (2007) 7164-7183.

[2] R.H. Venderbosch, A.R. Ardiyanti, J. Wildschut, A. Oasmaa, H.J. Heeres, Journal of Chemical Technology and Biotechnology. 85 (2010) 674-686.

[3] R.H. Venderbosch, W. Prins, Biofuels, Bioproducts and Biorefining. 4 (2010) 178-208.

[4] A. Oasmaa, E. Kuoppala, A.R. Ardiyanti, R.H. Venderbosch, H.J. Heeres, Energy Fuels. 24 (2010) 5264-5272.

[5] A. Oasmaa, D.C. Elliott, J. Korhonen, Energy Fuels. 24 (2010) 6548-6554.

[6] A. Oasmaa, E. Kuoppala, D.C. Elliott, Energy Fuels. 26 (2012) 2454-2460.

[7] A. Oasmaa, J. Korhonen, E. Kuoppala, Energy Fuels. 25 (2011) 3307-3313.

[8] H. Wang, J. Male, Y. Wang, ACS Catalysis. 3 (2013) 1047-1070.

[9] A.H. Zacher, M.V. Olarte, D.M. Santosa, D.C. Elliott, S.B. Jones, Green Chemistry. 16 (2014) 491-515.

[10] D.C. Elliott, Energy Fuels. 21 (2007) 1792-1815.

[11] F. Mercader, M. Groeneveld, S. Kersten, R. Venderbosch, J. Hogendoorn, Fuel. 89 (2010) 2829-2837.

[12] P.M. Mortensen, J. Grunwaldt, P.A. Jensen, K. Knudsen, A.D. Jensen, Applied Catalysis A: General. 407 (2011) 1-19.

[13] D.C. Elliott, T.R. Hart, G.G. Neuenschwander, L.J. Rotness, M.V. Olarte, A.H. Zacher, Y. Solantausta, Energy Fuels. 26 (2012) 3891-3896.

[14] D.C. Elliott, T.R. Hart, Energy Fuels. 23 (2008) 631-637.

[15] J. Wildschut, F.H. Mahfud, R.H. Venderbosch, H.J. Heeres, Industrial & Engineering Chemistry Research. 48 (2009) 10324-10334.

[16] W. Baldauf, U. Balfanz, M. Rupp, Biomass Bioenergy. 7 (1994) 237-244.

[17] A.R. Ardiyanti, A. Gutierrez, M. Honkela, A. Krause, H.J. Heeres, Applied Catalysis A: General. 407 (2011) 56-66.

[18] W. Wang, Y. Yang, J. Bao, Z. Chen, Journal of Fuel Chemistry and Technology. 37 (2009) 701-706.

[19] W. Wang, Y. Yang, H. Luo, T. Hu, W. Liu, Catalysis Communications. 12 (2011) 436-440.

[20] W. Wang, Y. Yang, H. Luo, H. Peng, F. Wang, Industrial & Engineering Chemistry Research. 50 (2011) 10936-10942.

[21] W. Wang, Y. Yang, H. Luo, H. Peng, B. He, W. Liu, Catalysis Communications. 12 (2011) 1275-1279.

[22] H. Zhao, D. Li, P. Bui, S. Oyama, Applied Catalysis A: General. 391 (2011) 305-310.

[23] A.R. Ardiyanti, S. Khromova, R.H. Venderbosch, V. Yakovlev, H.J. Heeres, Applied Catalysis B: Environmental. 117 (2012) 105-117.

[24] A. R. Ardiyanti, Ph.D. Thesis, University of Groningen, Groningen, the Netherlands, 2013; ISBN: 978-90-6182-234-5.

[25] A.R. Ardiyanti, M. Bykova, S. Khromova, W. Yin, R.H. Venderbosch, V.A. Yakovlev, H.J. Heeres, Energy Fuels. 30 (2016) 1544-1554.

[26] M. Bykova, D.Y. Ermakov, V. Kaichev, O. Bulavchenko, A. Saraev, M.Y. Lebedev, V. Yakovlev, Applied Catalysis B: Environmental. 113 (2012) 296-307.

[27] M. Bykova, D.Y. Ermakov, S. Khromova, A. Smirnov, M.Y. Lebedev, V. Yakovlev, Catalysis Today. 220-222 (2014) 21-31.

[28] V. Yakovlev, M. Bykova, S. Khromova, Catalysis in Industry. 4 (2012) 324-339.

[29] V. Yakovlev, S. Khromova, O. Sherstyuk, V. Dundich, D.Y. Ermakov, V. Novopashina, M.Y. Lebedev, O. Bulavchenko, V. Parmon, Catalysis Today. 144 (2009) 362-366.

[30] A.R. Ardiyanti, S. Khromova, R.H. Venderbosch, V. Yakovlev, I. Melián-Cabrera, H.J. Heeres, Applied Catalysis A: General. 449 (2012) 121-130.

[31] A. Kloekhorst, H.J. Heeres, ACS Sustainable Chemistry & Engineering. 3(2015) 1905–1914.

[32] A. Kloekhorst, J. Wildschut, H.J. Heeres, Catalysis Science & Technology. 4 (2014) 2367-2377.

[33] C.R. Kumar, N. Anand, A. Kloekhorst, C. Cannilla, G. Bonura, F. Frusteri, K. Barta, H.J. Heeres, Green Chemistry. 17(2015) 4921-4930.

[34] W. Yin, A. Kloekhorst, R.H. Venderbosch, M.V. Bykova, S.A. Khromova, V.A. Yakovlev, H.J. Heeres, Catalysis Science & Technology. 6(2016) 5899-5915.

[35] M.D. Navalikhina, O.V. Krylov, Russian Chemical Reviews. 67 (1998) 587-616.

[36] G.W. Huber, R.D. Cortright, J.A. Dumesic, Angewandte Chemie International Edition. 43 (2004) 1549-1551.

[37] W. Yin, R. H. Venderbosch, M. V. Bykova, H. Heeres, S. A. Khromova, V. A. Yakovlev, C. Cannilla, G. Bonura, F. Frusteri, Hero J. Heeres, Submitted to Applied Catalysis B: Environmental (2016).

[38] D. C. Elliott, J. Hu, T. R. Hart, G. G. Neuenschwander, Patent International, 7425657, 2008.

[39] F. de Miguel Mercader, M.J. Groeneveld, S.R. Kersten, C. Geantet, G. Toussaint, N.W. Way, C.J. Schaverien, K.J. Hogendoorn, Energy & Environmental Science. 4 (2011) 985-997.

[40] P. Ghetti, Fuel. 73 (1994) 1918-1921.

[41] F. Noel, Fuel. 63 (1984) 931-934.

[42] L. Ingram, D. Mohan, M. Bricka, P. Steele, D. Strobel, D. Crocker, B. Mitchell, J. Mohammad, K. Cantrell, C.U. Pittman Jr, Energy Fuels. 22 (2007) 614-625.

[43] C.A. Mullen, G.D. Strahan, A.A. Boateng, Energy Fuels. 23 (2009) 2707-2718.

[44] A. Kloekhorst, H.J. Heeres, Catalysis Science & Technology. 6(2016) 7053-7067.

[45] London metal exchange, www.lme.com (accessed Sept 2016).